

PHYSICAL REVIEW C

NUCLEAR PHYSICS

THIRD SERIES, VOLUME 56, NUMBER 5

NOVEMBER 1997

RAPID COMMUNICATIONS

The Rapid Communications section is intended for the accelerated publication of important new results. Manuscripts submitted to this section are given priority in handling in the editorial office and in production. A Rapid Communication in **Physical Review C** may be no longer than five printed pages and must be accompanied by an abstract. Page proofs are sent to authors.

Measurements of electromagnetic decay strengths in ^{92}Ru with cluster detectors

C. Lingk, A. Jungclauss, D. Kast, K. P. Lieb, C. Teich, and M. Weiszflog*

II. Physikalisches Institut, Universität Göttingen, Bunsenstrasse 7-9, D-37073 Göttingen, Germany

C. Ender, T. Härtlein, F. Köck, and D. Schwalm

Max-Planck Institut für Kernphysik, D-69029 Heidelberg, Germany

A. Dewald, J. Eberth, R. Peusquens, and H. G. Thomas

Universität zu Köln, Zùlpicher Str. 77, D-50937 Köln, Germany

M. Górska and H. Grawe

Gesellschaft für Schwerionenforschung, D-64291 Darmstadt, Germany

(Received 9 July 1997)

High-spin states in ^{92}Ru were populated via the reaction $^{58}\text{Ni}(^{40}\text{Ca}, \alpha 2p)$ at 145 MeV beam energy. Using six EUROBALL cluster detectors we measured lifetimes by means of the recoil distance Doppler shift method and are able to propose several significant changes in the published level scheme of ^{92}Ru . While the observed spin dependence of $M1$ - and moderately enhanced $E2$ -strengths is well reproduced by the shell model in the parametrization by Gross and Frenkel, the use of a surface delta residual force leads to less satisfactory results. [S0556-2813(97)50511-5]

PACS number(s): 21.10.Tg, 23.20.Lv, 25.70.Gh, 27.60.+j

Recent studies have shown that simple shell model calculations with only the $g_{9/2}$ and $p_{1/2}$ proton and neutron shells active can explain many experimental facets of $Z \leq 50$ nuclei near the $N = 50$ shell closure [1]. While a surface delta residual force [2] works about as well for the energies of the yrast and yrare levels as the set of empirical two-body matrix elements deduced by Gross and Frenkel [3], the latter approach much better reproduces, on average, the distribution of $M1$ and $E2$ γ -ray strengths. However, the agreement becomes worse when approaching the $N = 46$ borderline to the quadrupole deformed region [1,4–7]. As the effective shell model parameters [3] have been fitted by taking ^{88}Sr ($Z=38$, $N=50$) as the core, it is not *a priori* clear how successful this approach is when increasing Z and approaching ^{100}Sn [8].

Therefore we have started a systematic study of $N \leq 50$ Ru, Rh, and Pd nuclei ($Z=44$ –46).

The high-spin spectrum of the $Z=44$, $N=48$ nucleus ^{92}Ru has previously been studied by Nolte *et al.* [9] and by Arnell *et al.* [10]. Their ‘tentative’ level scheme features several irregularities in the level ordering typical of pairing effects: low- and high-energy transitions follow each other, giving rise to nanosecond isomers and making it difficult to order the γ rays in the level scheme according to their intensities. The primary motivation of the present lifetime measurements in ^{92}Ru by means of the recoil distance Doppler shift (RDDS) technique was to determine the absolute $M1$ and $E2$ transition strengths and their spin dependence. The use of six highly efficient EUROBALL cluster detectors [11] allowed us to measure the lifetimes in the $\gamma\gamma$ -coincidence mode with appropriate gating conditions, which also led to significant revisions in the published level scheme [10].

The experiment was performed by means of the reaction $^{58}\text{Ni}(^{40}\text{Ca}, \alpha 2p)^{92}\text{Ru}$ using a 3-pnA 145 MeV $^{40}\text{Ca}^{10+}$ beam

*Present address: The Svedberg Laboratory, Uppsala University, Box 553, S-75121 Uppsala, Sweden.

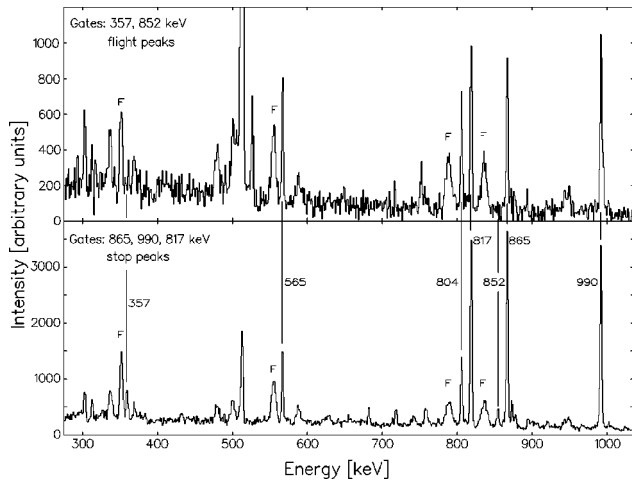


FIG. 1. Typical spectra with gates set on flight and stopped components as indicated (distance: 1000 μm).

provided by the Heidelberg MP-tandem accelerator. The plunger apparatus consisted of a 1.0 mg/cm² stretched ⁵⁸Ni foil (enrichment 99.9%) and a 16.6 mg/cm² stretched Ta stopper foil. Data were taken for 17 distances ranging from 15 μm to 10 mm, corrected for an offset of 12(2) μm . Each flight distance was set with a piezoelectric linear motor and checked via a piezo-feedback system and the capacitance of the target-stopper system. For comparison, data were also taken at zero flight distance by using a 300 mg/cm² gold-backed ⁵⁸Ni target. In these spectra, no Doppler broadened line shapes were observed, which would indicate effective lifetimes below 0.5 ps. The γ radiation was detected in six cluster detectors [11] arranged symmetrically around the beam axis in two groups of three detectors at 41° and 139°, respectively. This 2 \times 3-cluster setup offers favorable conditions for Doppler-shift measurements, as for each direction the data from all three cluster detectors, which were run in add-back mode [11], were added, giving a total photopeak efficiency of 5.9%. Summed spectra gated on the 865, 990, and 817 keV transitions (stop peak) and the 357 and 852 keV transitions (flight peak) are illustrated in Fig. 1.

In most cases, the decay functions were analyzed with the conventional RDDS approach [12] by setting coincidence gates on the 817, 990, and 865 keV transitions below the isomeric ($\tau=144(20)$ ns [9]) 2834 keV (8^+) state, which have only stopped components, thus selecting the relatively weak ⁹²Ru reaction channel ($\approx 10\%$ of the total fusion cross section). The correct feeding patterns, as deduced from the γ -ray intensities, were taken into account. In some rare cases finite sidefeeding times $\tau_{\text{SF}}=2-5$ ps had to be assumed in order to improve the fits. For several states, spectra in coincidence with the flight components of short-lived discrete feeders could be created to apply the differential decay curve method (DDCM) [13].

As mentioned in [10], in some cases it was not possible to fix the level order in ⁹²Ru solely on the basis of γ -ray intensities (with uncertainties due to close-lying doublets) without any additional information such as the observation of cross transitions. Figure 2 shows the relevant part of the level scheme of ⁹²Ru taken from [10], but modified according to the results of the present experiment. Changes were made in the level orderings involving the three γ -ray sequences of

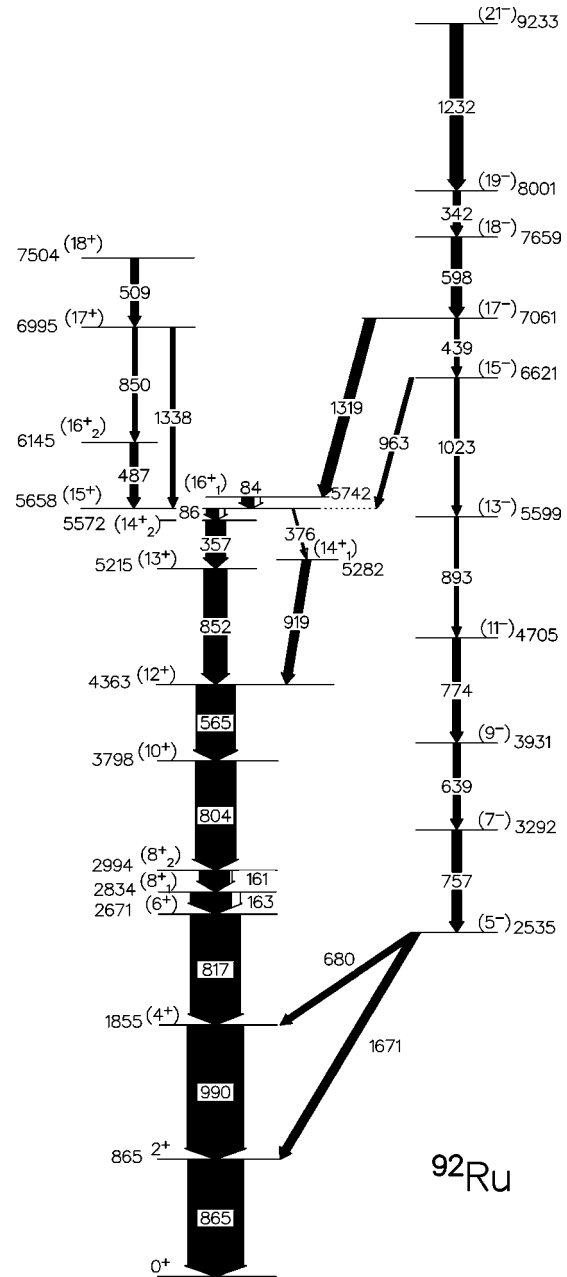


FIG. 2. Relevant part of the level scheme of ⁹²Ru from the work of Arnell *et al.* [10], modified according to the results of the present study (see text for details).

161-804-565 keV, 757-639-774 keV, and 84-1319 keV, respectively. Coincidence recoil distance data can provide direct information concerning this point: the occurrence of stopped and/or flight components in coincidence with those of one of the other γ rays in the cascade defines the order, i.e., it would be a contradiction to observe a flight component of a subsequent transition in coincidence with the stopped component of the preceding one. With this method the first two of the sequences mentioned above have been reordered.

In the case of the 84-1319 keV cascade, the RDDS data indicate a reversal in a less direct way. In the previous work [10], the 84 keV transition was placed to depopulate the (17^-) level at 7061 keV, leading to a tentative (16^-) state at 6977 keV. In Fig. 3, the decay curves $R(d)$ of the stopped components of the transitions with 439, 1319, 357, and 852

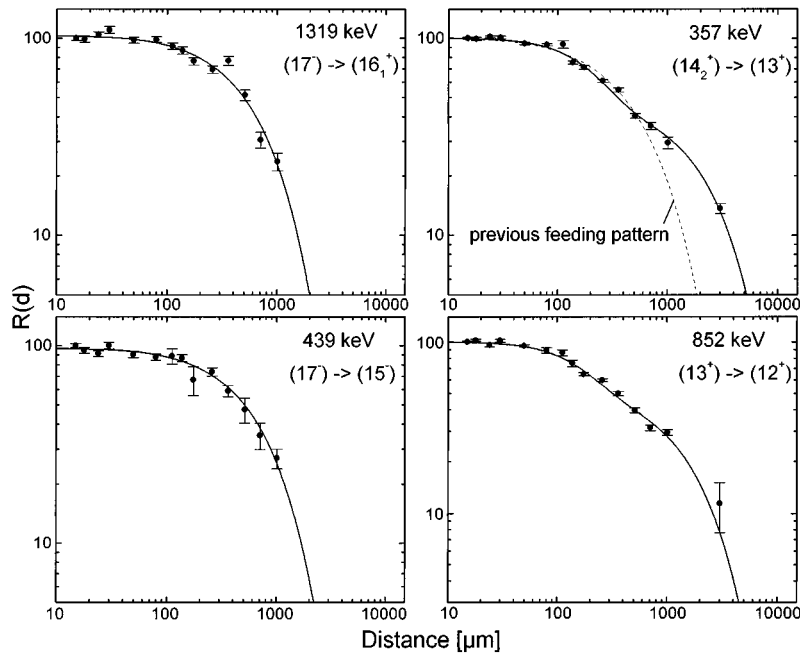


FIG. 3. Decay curves $R(d)$ of the 439, 1319, 357, and 852 keV transitions. The dashed line indicates the decay function expected for the 357 keV line assuming a feeding pattern corresponding to the level order suggested in [10].

keV, relevant for the following discussion, are shown. The decay functions of the 84/86 keV doublet could not be extracted. The decay curves of the 1319 and 439 keV transitions both yield a lifetime of $\tau=79(5)$ ps for the 7061 keV (17^-) state, taking into account the fast feeding via the 1232-342-598 keV cascade. According to the previous level ordering, the decay curve of the 357 keV transition would have to be described with two nearly equally strong feeding components, one from the short-lived (16_2^+) and (17^+)

feeder states (<2 ps) and one from the (17^-) level with $\tau=79(5)$ ps. However, applying this feeding pattern, the decay curve cannot be described, as demonstrated in Fig. 3. To reproduce the experimental data, a longer feeding component is required. The same is true for the decay function of the 852 keV transition. Due to this fact, we suggest that the 1319 keV γ -ray depopulates the (17^-) state, leading to a (16_1^+) level at 5742 keV, which is depopulated by the 84 keV transition. The long feeding necessary to describe the experimen-

TABLE I. Summary of lifetimes and transition strengths determined in ^{92}Ru .

E_x (keV)	I^π	τ (ps)	$I_i^\pi \rightarrow I_f^\pi$	E_γ (keV)	I_γ (%)	$B(M1)$ (mW.u.)	$B(E2)$ (W.u.)
2994	(8_2^+)	<18	(8_2^+) \rightarrow (8_1^+)	161 ^b	80.2(10)	>390	
3798	(10^+)	6.7(35)	(10^+) \rightarrow (8_2^+)	804	100.0(8)		14.7(77)
4363	(12^+)	79(6)	(12^+) \rightarrow (10^+)	565	95.6(8)		7.3(6)
5215	(13^+)	<2	(13^+) \rightarrow (12^+)	852	55.6(9)	>26	
5282	(14_1^+)	<10	(14_1^+) \rightarrow (12^+)	919	20.5(12)		>5
5572	(14_2^+)	<2	(14_2^+) \rightarrow (13^+)	357 ^b	46.9(9)	>345	
5658	(15^+)	14.5(48)	(15^+) \rightarrow (14_2^+)	86 ^b	46.9(9) ^c	2106(707)	
			(15^+) \rightarrow (14_1^+)	376 ^b	4.2(4)	3.6(14)	
5742	(16_1^+)	200(80)	(16_1^+) \rightarrow (15^+)	84 ^b	—	177(71)	
3292	(7^-)	23(7)	(7^-) \rightarrow (5^-)	757	22.2(7)		5.8(18)
3931	(9^-)	<5	(9^-) \rightarrow (7^-)	639	17.3(7)		>62
4705	(11^-)	15.7(42)	(11^-) \rightarrow (9^-)	774	18.3(4)		7.6(21)
5599	(13^-)	<2	(13^-) \rightarrow (11^-)	893	9.0(5)		>23
6621	(15^-)	<2	(15^-) \rightarrow (13^-)	1023	10.4(7)		>11
7061	(17^-)	79(5)	(17^-) \rightarrow (15^-)	439	11.8(9)		8.5(8)
7659	(18^-)	<1	(18^-) \rightarrow (17^-)	598	24.1(10)	>140	
8001	(19^-)	<1	(19^-) \rightarrow (18^-)	342 ^b	16.6(10)	>785	
9233	(21^-)	3.5(4) ^a	(21^-) \rightarrow (19^-)	1232	30.3(19)		>2.9

^aEffective lifetime.

^bCorrected for electron conversion according to [21].

^cAssuming no sidefeeding into the 14_2^+ state.

tal decay curves of the 357 keV and 852 keV transitions would then originate from this state. The sum of the lifetimes of the (15^+) and the (14_2^+) states was determined to be $\tau=14.5(48)$ ps via the DDCM method. Due to the small transition energy of 86 keV, this lifetime is likely to belong to the (15^+) level, whereas the lifetime of the (14_2^+) state is short (<2 ps).

Based on the measured decay functions, we obtained the lifetimes and transition strengths—or their limits—summarized in Table I. Nolte *et al.* [9] determined an effective lifetime of 124(13) ps for the 804 and 565 keV γ rays which we can now attribute to the lifetime of the 4363 keV state. One notes that the decay functions are dominated by the long lifetimes of few yrast states at 4363 keV [(12^+) , 79(6) ps], 5742 keV [(16_1^+) , ≈ 200 ps], and 7061 keV [(17^-) , 79(5) ps]. For that reason, the shorter lifetimes of the intermediate states were not accessible at all or could only be deduced with large errors. Finally, the 2535 keV (5^-) level does not decay within the flight path of 10 mm, leading to a lifetime limit of $\tau > 1.5$ ns, in agreement with the known value $\tau(5^-) = 23(3)$ ns [14].

The measured $M1$ and $E2$ transition strengths will now be compared with the predictions of the shell model, based on the truncation of the model space to $g_{9/2}$ and $p_{1/2}$ for protons and neutrons and the single-particle energies and two-body matrix elements according to Gross and Frenkel (GF) [3]. Details of these calculations, which were performed with the computer code RITSSCHIL [15], have been given in several previous papers, in particular for high-spin states in the $N=48$ isotones ^{89}Nb [16], ^{90}Mo [7,17,18], and ^{91}Tc [1], as well as in the neighboring Ru isotopes $^{90,91}\text{Ru}$ [19]. For comparison, we also present the results of calculations done with two-body matrix elements calculated with a surface delta residual force (SD) [2]. In Fig. 4, the measured $M1$ and $E2$ strengths are summarized in comparison with the theoretical values labeled GF and SD. Both parametrizations give very similar predictions of the $M1$ strengths (≈ 1 W.u.) for all the transitions, except the $15_1^+ \rightarrow 14_1^+$ transition. Interestingly, both GF and SD support the very large $B(M1)$ of the $15_1^+ \rightarrow 14_2^+$ transition (2 W.u.), but disagree in their predictions of the strongly reduced $B(M1)$ of the $15_1^+ \rightarrow 14_1^+$ transition (3.6 mW.u.), which is better reproduced by SD (2 mW.u.) than by GF (100 mW.u.). Looking at the calculated wave functions listed in Table II, one notes, indeed, the large overlap between the 15^+ and 14_2^+ configurations in both calculations: the main components only differ by the total spins to which the $v_\pi=2$, $I_\pi=8$ proton part and the $v_\nu=2$, $I_\nu=8$ neutron part do couple. In contrast to this, the very different configuration of the 14_1^+ state only allows for a very weak $15_1^+ \rightarrow 14_1^+$ $M1$ strength. We have identified similar groupings of $M1$ strengths in $^{88,90}\text{Mo}$ [7] and ^{90}Tc [1,20]. In each of these nuclei, a class of several large (≈ 1 W.u.) and another class of a few small $M1$ transitions (≈ 20 mW.u.) have been encountered. Concerning the $E2$ strengths in ^{92}Ru also presented in Fig. 4, the GF values are concentrated around 10 W.u., while the SD values scatter over two orders of magnitude. This is a consequence of the fact that SD over-emphasizes rapid changes of seniority at spin values which can be reached only by breaking one additional pair of nucleons. The GF wave functions, on the other hand, are more

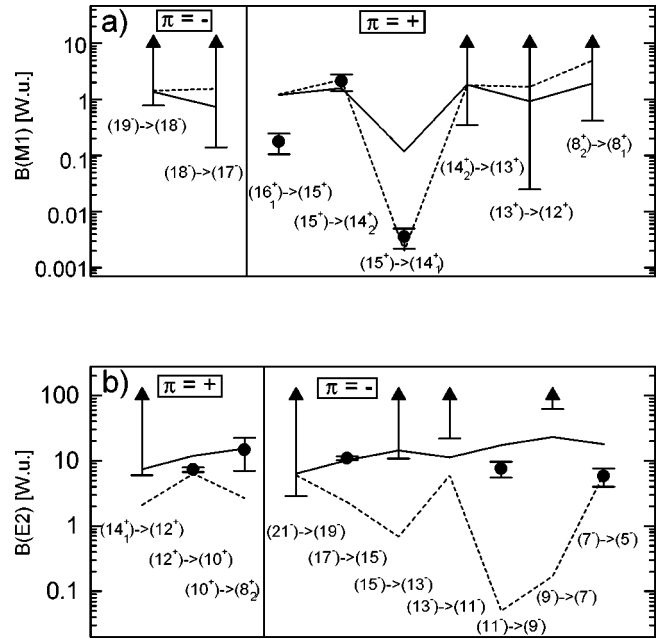


FIG. 4. Comparison between experimental and theoretical transition strengths in ^{92}Ru for (a) $M1$ transitions and (b) $E2$ transitions. The solid lines indicate the values calculated using the GF parameters, the dashed lines represent the results obtained with the SD interaction.

strongly mixed in seniority [1]. The measured $E2$ strengths agree with the GF values or are much closer to them and are not compatible with the fluctuating $E2$ strengths predicted by SD.

To summarize, the present coincidence recoil distance lifetime experiment in ^{92}Ru has profited from the large efficiency of the new EUROBALL cluster detectors, which allowed us to overcome the difficulties of the previous $\gamma\gamma$ -coincidence study [10]. On the basis of the present experiment, we consider the coincidence recoil distance technique not only as necessary to measure ps lifetimes in weakly populated nuclei, but also to establish level orders in high-spin cascades of shell model structure having irregular patterns of low-energy and high-energy transitions. In ^{92}Ru , we measured 10–100 ps lifetimes and proposed three signifi-

TABLE II. Main partitions of the wave functions of the 15^+ , 14_1^+ , and 14_2^+ states.

State	Partition	GF (%)	SD (%)
15^+	$\pi_8^2 \nu_8^{-2}$	73.7	80.1
	$\pi_7^4 \nu_8^{-2}$	12.1	3.7
14_2^+	$\pi_8^2 \nu_8^{-2}$	43.1	78.9
	$\pi_8^2 \nu_6^{-2}$	17.2	2.0
	$\pi_7^4 \nu_8^{-2}$	15.1	3.4
	$\pi_8^2 \nu_8^{-2}$	3.0	2.0
	$\pi_6^4 \nu_8^{-2}$	1.3	0.8
	$\pi_8^2 \nu_8^{-2}$	4.1	0.04
14_1^+	$\pi_8^2 \nu_8^{-2}$	22.0	37.8
	$\pi_7^4 \nu_8^{-2}$	1.8	0.7
	$\pi_6^2 \nu_8^{-2}$	37.5	38.8
	$\pi_6^4 \nu_8^{-2}$	20.2	5.9

cant changes to the previously published level scheme. The transition strengths are, on average, well reproduced by the shell model approach with Gross-Frenkel parameters, which are superior to the surface delta interaction matrix elements. The most relevant result of this work refers to the decay of the 15^+ yrast state to the 14^+ yrast and yrare states, via $M1$ transitions differing in strength by more than two orders of

magnitude. These two $B(M1)$ values, indeed, nicely support the shell model structures.

We are most grateful to Dr. Repnow and the crew of the Heidelberg tandem accelerator for their friendly and efficient cooperation. The EUROBALL project is being funded by Deutsches Bundesministerium für Bildung, Wissenschaft, Forschung und Technologie (BMBF).

-
- [1] D. Rudolph, K. P. Lieb, and H. Grawe, Nucl. Phys. **A597**, 298 (1996); D. Rudolph *et al.*, Phys. Scr. **T56**, 120 (1995).
- [2] A. Plastino *et al.*, Phys. Rev. **145**, 837 (1966).
- [3] R. Gross and A. Frenkel, Nucl. Phys. **A267**, 85 (1976).
- [4] A. Jungclaus *et al.*, Z. Phys. A **340**, 125 (1991).
- [5] M. Weiszflog *et al.*, Z. Phys. A **342**, 257 (1992); Nucl. Phys. **A584**, 133 (1995).
- [6] P. Chowdhury *et al.*, Phys. Rev. Lett. **67**, 2950 (1991); A. A. Chishti *et al.*, Phys. Rev. C **48**, 2607 (1993).
- [7] M. Kabadiyski *et al.*, Phys. Rev. C **50**, 110 (1994).
- [8] H. Grawe *et al.*, Acta Phys. Pol. B **26**, 341 (1995); Phys. Scr. **T56**, 71 (1995).
- [9] E. Nolte, G. Korschinek, and U. Heim, Z. Phys. A **298**, 191 (1980).
- [10] S. E. Arnell *et al.*, Z. Phys. A **346**, 111 (1993).
- [11] J. Eberth *et al.*, Nucl. Instrum. Methods Phys. Res. A **369**, 135 (1996).
- [12] D. B. Fossan and E. K. Warburton, in *Nuclear Spectroscopy and Reactions* Vol. C (Academic, New York, 1974); P. J. Nolan and J. F. Sharpey-Schafer, Rep. Prog. Phys. **42**, 1 (1979); K. P. Lieb, in *Modern Techniques in Nuclear Physics*, edited by D. Poenaru and W. Greiner (de Gruyter, Berlin, 1997).
- [13] A. Dewald *et al.*, Z. Phys. A **334**, 163 (1989); G. Boehm *et al.*, Nucl. Instrum. Methods Phys. Res. A **329**, 248 (1993).
- [14] M. Górska *et al.*, Acta Phys. Pol. B **27**, 165 (1996).
- [15] D. Zwarts, Comput. Phys. Commun. **38**, 365 (1985).
- [16] A. Bödeker *et al.*, Phys. Rev. C **48**, 1617 (1993); D. Zainea *et al.*, Z. Phys. A **352**, 365 (1995).
- [17] M. K. Kabadiyski *et al.*, Z. Phys. A **343**, 165 (1992); M. Weiszflog *et al.*, J. Phys. G **20**, L77 (1994).
- [18] S. E. Arnell *et al.*, Phys. Scr. **47**, 142 (1993); D. Rudolph *et al.*, Phys. Rev. C **49**, 66 (1994).
- [19] J. Heese *et al.*, Phys. Rev. C **49**, 1896 (1994).
- [20] D. Rudolph *et al.*, Z. Phys. A **349**, 105 (1994).
- [21] F. Rösler *et al.*, At. Data Nucl. Data Tables **21**, 91 (1978).